EPR Spectroscopy and Imaging of Free Radicals in Food

PHILIPPE P. LEVÊQUE, QUENTIN GODECHAL, AND BERNARD GALLEZ*
Biomedical Magnetic Resonance Unit, Université Catholique de Louvain, REMA 73-40, Avenue Mounier 73, B-1200, Brussels, Belgium

(Received 9 January 2008 and in revised form 22 February 2008)

Abstract. Electron Paramagnetic Resonance (EPR) is a well-known spectroscopic and imaging technique that can detect free radicals both in vitro and non-invasively in vivo, with high sensitivity. In food, free radicals can be generated by several commonly used industrial processes, such as radiosterilization or heat treatment. EPR spectroscopy has been widely used to detect radioinduced free radicals in food, but is limited to the measurement of the global response of a sample. EPR imaging (EPRI) allows the spin density distribution of free radicals to be mapped within objects. We investigated the possibility of acquiring 2D and 3D EPR images of the distribution of free radicals in various foodstuffs with naturally occurring or induced free radicals, including frogs' legs, tea leaves, coffee beans, and sunflower seeds.

Our results demonstrated that the free radicals contained in foodstuffs give EPR signals with characteristics compatible with the acquisition of high-quality images. Small-size structures (e.g., frog bones, 1.0–1.5 mm width) could be delineated with accuracy. The strongest signals came from irradiated samples, but low-intensity signals from naturally occurring free radicals could also be imaged. EPRI is likely to be used when additional information is needed about the spatial distribution of unpaired electrons. The method offers the unique ability to monitor the fate of these free radicals in biological samples and in vivo.

INTRODUCTION

Electron Paramagnetic Resonance (EPR), or Electron Spin Resonance (ESR), is a well-known spectroscopic and imaging technique that can detect free radicals both in vitro and non-invasively in vivo, with high sensitivity. In freely diffusing media, most free radicals are transient species that react very quickly with surrounding molecules and can hardly be detected without a specific technique such as spin trapping.[1] In solid state (or dry tissue), however, the lifetime of free radicals can be considerably longer, ranging from a few days to a few months or even years.[2]

In food, free radicals can be generated by several commonly used industrial processes such as heat treatment or irradiation by X- and γ-rays or accelerated electrons,[3] well-established procedures used to improve conservation shelf life or the microbiological quality of foodstuffs.[4,5] In the 1990s and early 2000s, numerous studies focused on the detection of irradiated food using EPR spectroscopy.[6–11] EPR signals distinguishable from non-irradiated material were observed in solid food or in the dry part of food, such as meat bones, fish bones, wheat seeds, sunflower and pumpkin fruits, stones or achenes of fresh fruits, dry fruits, spices, coffee beans, etc.[8] The shape of the EPR signal can be relatively simple, as in bones, where it appears as an asymmetric single line,[12–14] or have a more complex shape, depending on the type or part of foodstuff examined. EPR spectroscopy has been recognized by the European Committee for Standardization (CEN—Comité Européen de Normalisation) as the gold standard method for detecting irradiated food containing bones or cellulose.[15,16]

*Author to whom correspondence should be addressed.
E-mail: Bernard.Gallez@uclouvain.be

Spectroscopy, although a powerful tool, is limited to the measurement of the global response of a sample. In some situations, it may be necessary to study the spatial distribution of spin density within the object. This information can be provided by EPR imaging (EPRI), a modality of EPR that uses magnetic field gradients in a way similar to NMR imaging.[17,18] An additional set of field coils is used to generate a linear field gradient within the sample volume. When the main magnetic field is swept, the resonance condition will be different for each point located along the gradient line. A set of projections must be acquired at various angles according to the general principles of tomography. The image can then be reconstructed from backprojections.[18,19]

EPRI has been successfully applied to the detection of exogenous spin probes, but it remains difficult to perform imaging of endogenous free radicals because of their low concentration, instability, or rare occurrence. In this study, we investigated the possibility of acquiring 2D and 3D images of free radical distribution in various foodstuffs. We also discuss the general characteristics required to produce an image that unambiguously reflects spin density in this type of biological sample.

EXPERIMENTAL

Food Samples

The following samples of foodstuffs with low water content were acquired at the local supermarket: black, white, and green pepper (*Piper nigrum* sp.), pink pepper (*Shimus terebinthifolius*), and natural or roasted sunflower seeds (*Helianthus annus*). Green and black coffee beans and green and black tea leaves were obtained from a specialized shop, and pili pili pepper (*Capsicum frutescens* sp.) was a traditional preparation from the local market. Frozen frogs' legs were chosen as a sample of an irradiated foodstuff; they were freeze-dried under vacuum to remove water before imaging. Other food samples were measured without any treatment. The "Cachou" tablets, sweets made from various plant extracts, mainly licorice *(Glycyrrhiza glabra* L.*)*, came from Lajaunie (Toulouse, France).

EPR Spectrometer Settings

All spectra and images were acquired at room temperature on a Bruker E540 Elexsys system (Bruker Biospin GmBh, Karlsruhe, Germany), equipped with a Super High Sensitivity Probe also from Bruker (10 mm diameter, 30 mm long). The system was operated in X-band mode at ~9.5 GHz, 100 kHz modulation frequency. For imaging, the system was equipped with water-cooled gradients allowing a magnetic field gradient up to 49 G/cm along the X, Y, and Z axes.

For each sample, the microwave power was selected within the linear part of the power-√intensity curve. Amplitude modulation values were chosen so that they did not induce any signal distortion, and were always limited to the line width value. Conversion time, time constant, field sweep, and, for images, gradient intensity were optimized for each sample and are given in Table 1.

EPR Imaging

Samples were placed in a high-quality EPR quartz tube, which was positioned in the center of the microwave cavity. Images were acquired with different sample orientations or positions in order to verify anisotropic effects or field inhomogeneities. 2D and 3D images were reconstructed from a complete set of projections, collected as a function of the magnetic field gradient, using the backprojection algorithm implemented in the Xepr® software package from Bruker. Before reconstruction, the projections were deconvoluted with a zero-gradient line shape reference spectrum in order to improve resolution.

Table 1. Main EPR acquisition parameters

sample	field (G) (+ field sweep)	conversion time and time constant (ms)	amplitude modulation (G)	power (mW)	gradient (G/cm)	pixel size (mm)
frog's leg	3424 (275)	5.12 & 20.48	10	13	49	0.6 × 0.6
frog's leg isolated muscle	3424 (164)	5.12 & 20.48	10	13	34.1	0.6 × 0.6
green coffee	4000 (7000)	10.24 & 40.96	7	4.2	n/a	n/a
roasted coffee	3433 (93)	2.56 & 5.12	7	4.2	21	1.0 × 1.0
green tea	3440 (140)	10.24 & 10.24	3	2.6	34	0.6 × 0.6
sunflower	3444 (192)	10.24 & 5.12	7	2.6	49	0.8 × 0.8
pepper	3450 (124)	5.12 & 20.48	10	8.3	49	0.6 × 0.6
pili pili	3417 (234)	10.24 & 20.48	9	4.2	49	0.8 × 0.8
licorice sweet	3454 (138)	5.12 & 5.12	1.5	20.6	34	0.6 × 0.6

RESULTS

Frogs' Legs

The distal part of a frog's hind leg, irradiated at 15 kGy, gave a strong asymmetric EPR signal typical of the CO_3^- radical (LW = 11 G).[20] Another signal due to bone marrow (g = 2.0044) was also observed (data not shown). The images acquired in 2D and 3D mode (Fig. 1A) showed a rather homogeneous distribution of the spin density in the bone tissue. The calcaneus and astragalus bones were very well delineated; tarsal and metatarsal bones were visible but not resolved. Muscle tissue and the Achilles' tendon also gave a signal (g = 2.0081 and 2.0076), probably due to collagen, but much lower in intensity, so that they were not clearly visible with the conditions chosen to image the bones, but rather gave a general blurring of the image. Nevertheless, isolated muscle or tendon tissue could also be imaged separately with a longer accumulation time and more scans (Fig. 1B).

Coffee Beans

Roasted "black" coffee bean gave a strong EPR signal (g = 2.0028) that was absent in the green unroasted sample (Fig. 2B). It is assumed that this signal arises from semiquinone molecules (g = 2.0020).[21,22] The signal at low field was probably due to the Fe^{3+} radical and did not interfere with image acquisition. The overall shape and the measured distances on the image fit with the original values of the sample. Spin density distribution was heterogeneous, the center of the bean giving a greater intensity than the surrounding areas (Fig. 2A).

Tea Leaves

The spectral shape of tea samples varied quite a lot depending on batch provenance. In some instances, a broad (~500 G width) six line spectrum due to the Mn^{2+} radical was visible in both green and black tea (Fig. 3A). Superimposed on this Mn^{2+} signal, a single line shape peak was observed (g = 2.004, 6 G width), with a higher intensity in black tea. In this circumstance, images could

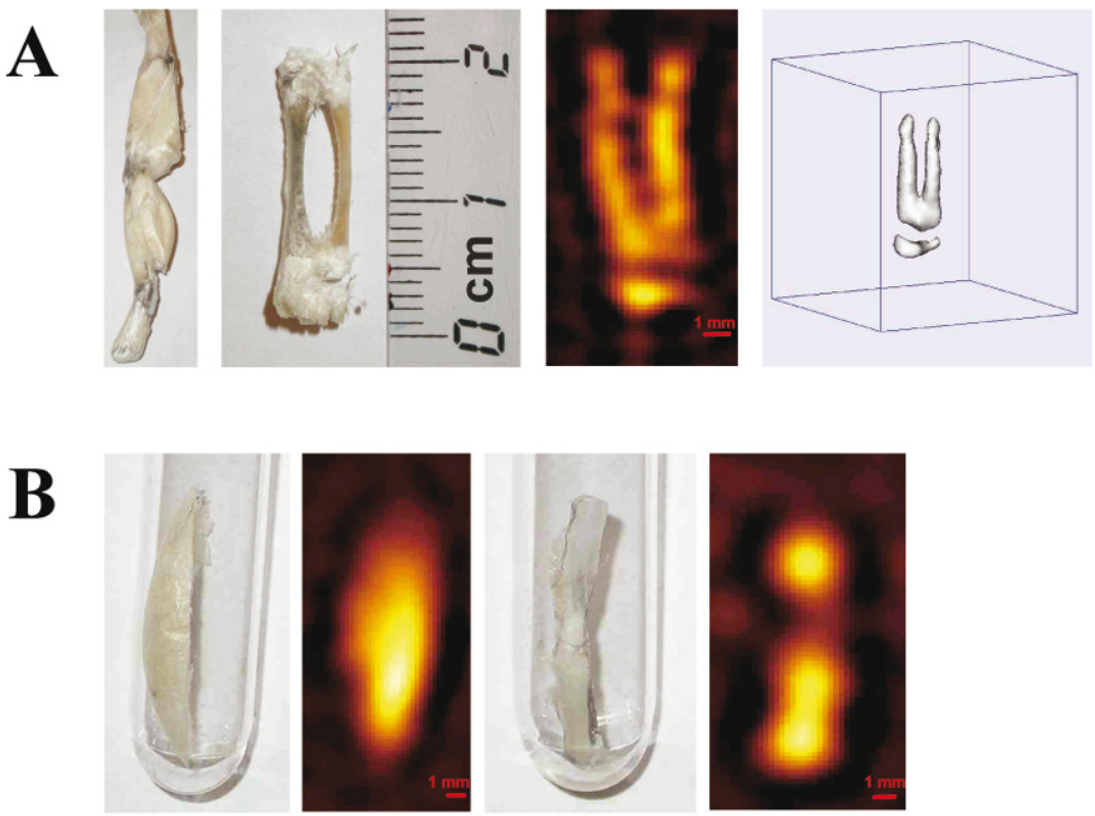

Fig. 1. (A) EPRI of irradiated frog's leg. *Far left*, view of the complete hind leg; only the distal part has been imaged. *Middle left*, skeleton after removing tissues. *Middle right*, EPRI 2D image of the leg. *Far right*, EPRI 3D surface view of spin density distribution. Pixel size 0.6 mm @ 49.1 G/cm. (B) Sample of isolated muscle tissue (*far left*) and the corresponding 2D EPRI view (*middle left*). Achilles' tendon (*middle right*) and its 2D EPR image (*far right*).

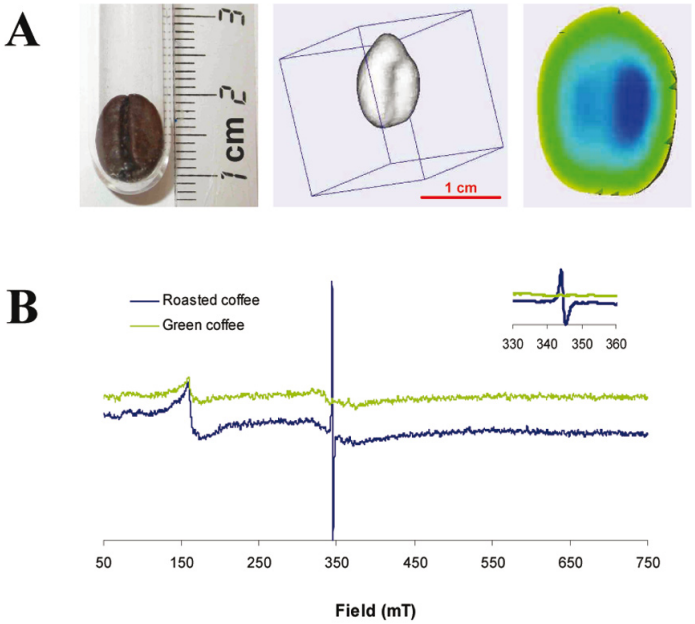

Fig. 2. (A) EPR image of roasted coffee bean. Original sample (*left*), 3D EPR surface view (*center*), and 3D EPR coronal slice view (*right*). Color scale: blue (highest intensity)>green>yellow (lowest intensity). (B) EPR spectra of green (green line) and black coffee bean (blue line).

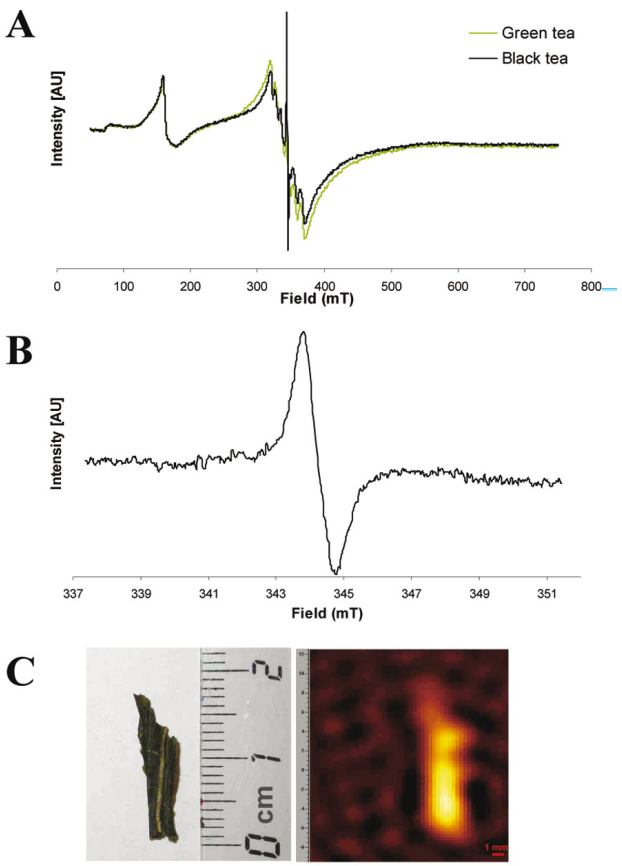

Fig. 3. (A) EPR spectrum of green and black tea. Central line g = 2.0044. Mn^{2+} lines (g = 1.874, 1.936, 1.979, 2.050, 2.100, and 2.147. (B) EPR spectrum of a green tea sample free of Mn^{2+} signal. (**C**) 2D EPRI image of a green tea leaf.

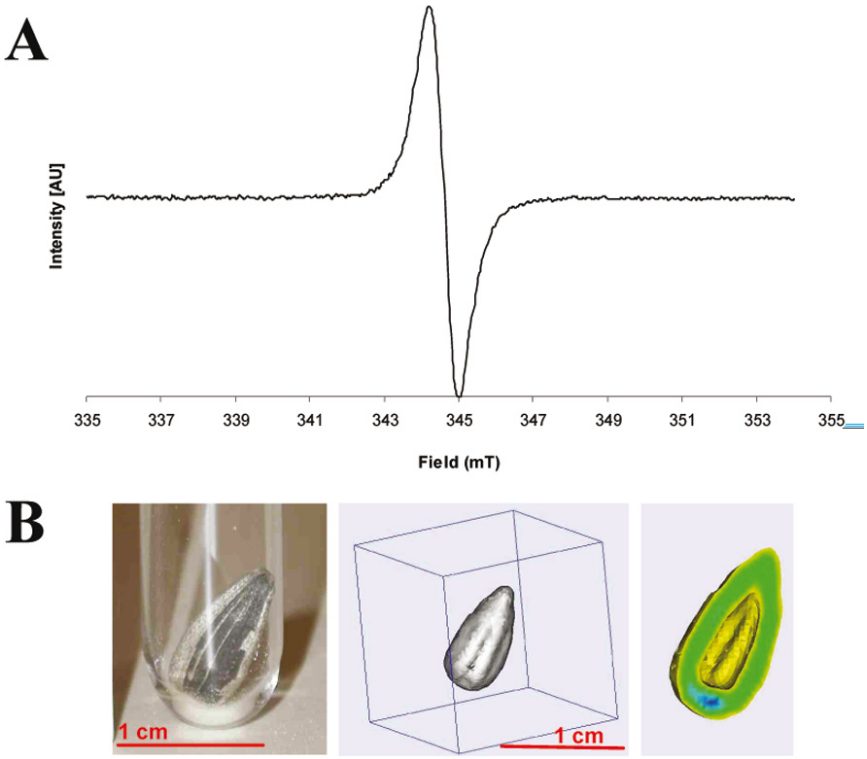

Fig. 4. (A) EPR spectrum of a sunflower fruit. (B) Original sunflower fruit (*left*), EPRI 3D surface image (*middle*), and a cross section view of spin density in the pericarp (*right*). Color scale: blue (highest intensity) > green > yellow (lowest intensity).

not be acquired due to Mn^{2+} interference. When Mn^{2+} was not present, in selected batches, the signal was composed of a single line (Fig. 3B) and it was possible to acquire an image although the intensity was very low, and reconstruction artefacts quite marked (Fig. 3C). No particular pattern was observed, the spin density distribution being globally homogeneous throughout the foliar limb. This EPR signal is reported to be due to stable radicals of aromatic origin, probably semiquinones produced by oxidation of phenolic compounds such as condensed tannins.[23,24] In black tea, oxidation is increased during the fermentation process.

Sunflower Seeds

Sunflower fruits are achenes composed of an external hard pericarp protecting the seed itself. We observed that the EPR signal came mainly from the pericarp, the seed giving only a very weak signal (roasted fruit) or no signal at all (natural untreated fruit). The signal from the seed (when present) and from the pericarp shared the same feature (Fig. 4A, single line g = 2.009), differing only in intensity. Spin density was uniformly distributed in the pericarp region, with a little hot spot at the base (Fig. 4B). The inner part of the fruit appeared empty as the seed had no or only a weak EPR signal.

Pepper

The spectra of peppercorns, normalized to sample weight, showed that black pepper had the most intense EPR signal. The weakest signal was observed for white pepper, whereas green pepper gave an intermediate intensity (Fig. 5). The 2D image of black peppercorns showed a signal distribution mainly in the external part of the fruit (pericarp), although the signal was not uniform within the pericarp. This is consistent with the low normalized signal recorded for white peppercorn, where the pericarp is removed. Black pepper is harvested when the fruit is almost ripe, berries are then fermented and dried. White pepper is the seed of the fruit obtained from fully ripened berries in which the pericarp has been mechanically removed. Green pepper is harvested a long time before the fruit is ripe, and kept moist. The origin of the signal is likely also due to quinone or semiquinone molecules naturally occurring in plants and also present in pepper.[22,25,26] On the other hand, it has been documented that heat treatment increases the signal in-

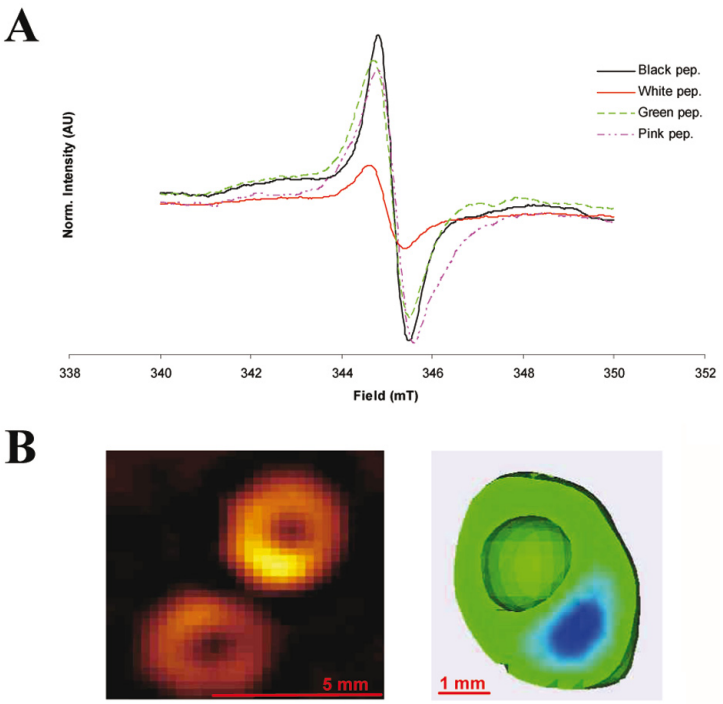

Fig. 5. (A) EPR spectrum of the various peppers, normalized to the sample weight. (B) 2D image of two black peppercorns, the signal arising from the external part of the fruit (*left*), and 3D view of a cross section through one peppercorn (*right*).

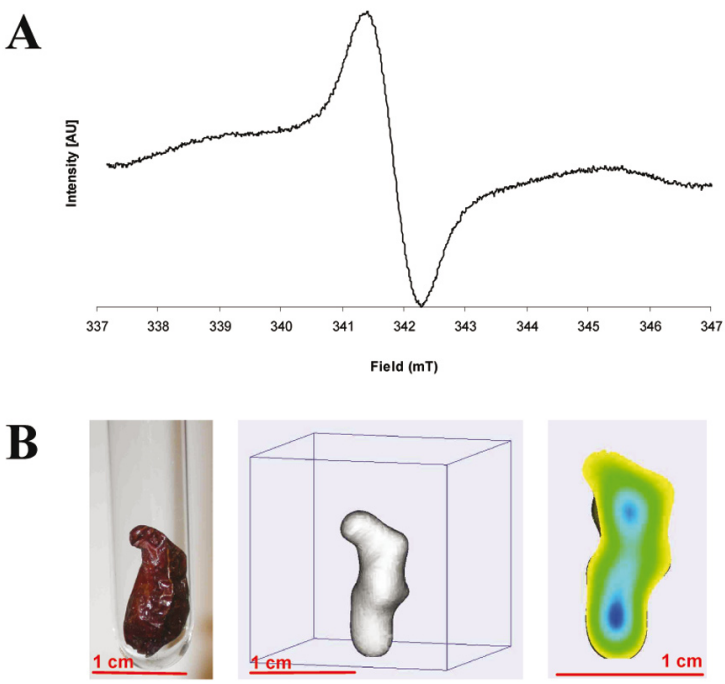

Fig. 6. (A) EPR spectrum of pili pili. (B) Original pili pili sample (*left*), 3D EPRI surface view (*middle*), and spin density distribution in a cross section through the center of the sample (*right*).

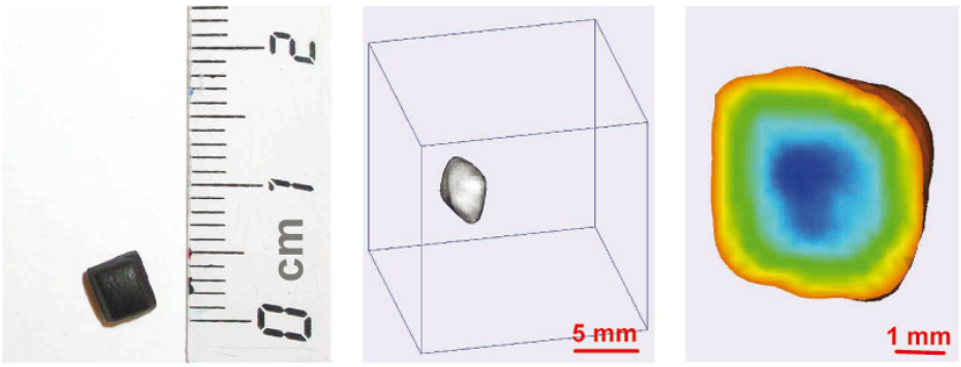

Fig. 7. "Cachou Lajaunie" tablet (*left*), 3D global surface view (*center*), and spin density distribution in a median cross section (*right*).

tensity recorded at this very g value. This line is attributed to peroxide radical formation by some authors.[27,28]

Pili Pili

The pili pili (*Capsicum frutescens* sp.) spectrum consisted of a singlet centered at g = 2.0108 (Fig. 6A). The origin of this signal is not known. In irradiated red pepper, a radioinduced EPR signal is observed and likely due to cellulose. Our sample was not gamma irradiated but only dried, so that the native signal likely arose from semiquinone radicals.

Licorice-Flavored Sweets

"Cachou" is a very old and well-known licorice-flavored sweet developed more than a century ago by a French pharmacist (Lajaunie) from Toulouse. It is made from various plant extracts but mainly licorice and arec nut. The presence of an EPR signal in "Cachou" was demonstrated by Gallez, and is characteristic of a high polyphenol content in licorice, which can be easily oxidized into radicals.[29] This strong signal allowed acquisition of 3D images showing a spin density gradient from the center to the edges of the tablet (Fig. 7).

DISCUSSION

EPR is a sensitive technique for the detection of unpaired electrons and has already been used in its spectroscopic modality to study free radicals in foodstuffs. EPRI remains to be investigated in this family of samples. Although EPR is more sensitive than NMR for the same concentration of spins, the natural concentration of unpaired electrons in biological samples is far less than that of protons, so that adequate signal-to-noise ratio is often a real concern. This is particularly important in EPRI where one must record the signal from each individual point (or projection) rather than for the sample as a whole. Imaging samples with satisfactory resolution requires that demanding conditions be satisfied. High resolution can be achieved by using a stronger field gradient, which in turn may cause signal distortions, possible deconvolution difficulties, and eventually a decrease in the signal-to-noise ratio. High resolution also necessitates a large sampling rate, i.e., increasing the number of projection angles during the acquisition. This process can decrease the signal intensity in each projection and may cause poor overall image quality. Finally, line width is also a great concern since a large line width decreases the resolution.

In this study, we investigated the possibility of imaging biological samples, like foodstuffs, where unpaired radicals can be present naturally or induced by industrial processes, such as fermentation and heat treatment or radiosterilization.

In our opinion, the best result was probably obtained in the radiosterilized frogs' legs, where radiation created a strong signal. It was possible to acquire a detailed picture of small structures, such as hind-leg bones, the width of which varies between 1.0 and 1.5 mm, despite an unfavorably wide EPR signal (~1 mT). 2D images could be recorded very rapidly in less than 15 minutes. However, in certain circumstances (e.g., green tea leaves), image acquisition was hindered by large spectral components arising from the presence of other paramagnetic species, such as Mn^{2+}. In between these two extremes, the EPR signal observed in the selected samples met the conditions to build images that reflected spin density distribution in relatively small structures.

This study demonstrates the ability of EPR to provide qualitative and quantitative information regarding spin distribution and free radical localization in biological samples such as foodstuffs.

CONCLUSIONS

We have demonstrated for the first time that EPRI can be applied to foodstuffs to study unpaired electron distribution in these biological samples. Free radicals, either naturally occurring, radio-, or thermo-induced, give an EPR signal, the characteristics of which are compatible with the acquisition of high-quality 2D and 3D images. As spectroscopy has been widely investigated in this particular field of the food industry, EPRI is likely to be used when additional information is needed about the spatial distribution of free radicals. The method offers unique capabilities to monitor the fate of these free radicals in biological samples in vivo.

REFERENCES AND NOTES

(1) Berliner, L.J.; Khramtsov, V.; Fujii, H.; Clanton, T.L. *Free Radical Biol. Med.* **2001**, *30*, 489–499.
(2) Ikeya, M.; Miki, T. *Science* **1980**, *207*, 977–979.
(3) Pilbrow, J.R.; Troup, G.J.; Hutton, D.R.; Rosengarten, G.; Zhong, Y.C.; Hunter, C.R. *Appl. Radiat. Isot.* **1993**, *44*, 413–417.
(4) Mahapatra, A.K.; Muthukumarappan, K.; Julson, J.L. *Crit. Rev. Food Sci. Nutr.* **2005**, *45*, 447–461.
(5) Parnes, R.B.; Lichtenstein, A.H. *Nutr. Clin. Care* **2004**, *7*, 149–155.
(6) Boegl, K.W. *Appl. Radiat. Isot.* **1989**, *40*, 1203–1210.
(7) Boegl, K.W. *Radiat. Phys. Chem.* **1990**, *35*, 301–310.
(8) Desrosiers, M.F. *Appl. Radiat. Isot.* **1996**, *47*, 1621–1628.
(9) Douifi, L.; Raffi, J.; Stocker, P.; Dole, F. *Spectrochim. Acta, Part A Mol. Biomol. Spectrosc.* **1998**, *54A*, 2403–2412.
(10) Raffi, J.; Belliardo, J.J.; Agnel, J.P.; Vincent, P. *Appl. Radiat. Isot.* **1993**, *44*, 407–412.
(11) Shimoyama, Y.; Ukai, M.; Nakamura, H. *Radiat. Phys. Chem.* **2007**, *76*, 1837–1839.
(12) Strzelczak, G.; Sadlo, J.; Danilczuk, M.; Stachowicz, W.; Callens, F.; Vanhaelewy, G.; Goovaerts, E.; Michalik, J. *Spectrochim. Acta, Part A Mol. Biomolec. Spectrosc.* **2007**, *67A*, 1206–1209.
(13) Stachowicz, W.; Burlinska, G.; Michalik, J.; Dziedzic-Goclawska, A.; Ostrowski, K. *Nukleonika* **1993**, *38*, 67–82.
(14) Callens, F.; Vanhaelewyn, G.; Matthys, P.; Boesman, E. *Appl. Magnet. Reson.* **1998**, *14*, 235–254.
(15) CEN EN Protocol EN 1786. Detection of irradiated food containing bone: analysis by electron paramagnetic resonance; European Committee for Standardization, Brussels, 1997.
(16) CEN EN Protocol EN 1787. Determination of irradiated food containing cellulose: analysis by EPR; European Committee for Standardization, Brussels, 2000.
(17) Kuppusamy, P.; Chzhan, M.; Zweier, J.L. *Biol. Magnet. Res.* **2003**, *18*, 99–152.
(18) Eaton, G.R.; Eaton, S.S.; Ohno, K. *EPR Imaging and In Vivo EPR*; CRC Press: Boca Raton, FL, 1991.
(19) Callaghan, P.T. *Principles of Nuclear Magnetic Resonance Microscopy*; Clarendon Press: Oxford, 1991.
(20) Raffi, J.; Evans, J.C.; Agnel, J.P.; Rowlands, C.C.; Lesgards, G. *Int. J. Radiat. Appl. Instrum. Part A* **1989**, *40*, 1215–1218.
(21) Bhushan, B.; Bhat, R.; Rao, B.Y.K.; Ahmad, R.; Bongirwar, D.R. *Int. J. Food Sci. Technol.* **2003**, *38*, 11–16.
(22) Raffi, J.J.; Agnel, J.P.L. *Radiat. Phys. Chem.* **1989**, *34*, 891–894.
(23) Morsy, M.A.; Khaled, M.M. *Spectrochim. Acta Part A: Molec. Biomolec. Spectrosc.* **2002**, *58*, 1271–1277.
(24) Polovka, M.; Brezova, V.; Stasko, A. *Biophys. Chem.* **2003**, *106*, 39–56.
(25) Polovka, M.; Brezova, V.; Stasko, A.; Mazur, M.; Suhaj, M.; Simko, P. *Radiat. Phys. Chem.* **2006**, *75*, 309–321.
(26) Calucci, L.; Pinzino, C.; Zandomeneghi, M.; Capocchi, A.; Ghiringhelli, S.; Saviozzi., F.; Tozzi, S.; Galleschi, L. *J. Agric. Food Chem.* **2003**, *51*, 927–934.
(27) Franco, R.W.A.; Martin-Neto, L.; Kato, M.S.A.; Furlan, G.R.; Walder, J.M.M.; Colnago, L.A. *Int. J. Food Sci. Technol.* **2004**, *39*, 395–401.
(28) Raffi, J.; Yordanov, N.D.; Chabane, S.; Douifi, L.; Gancheva, V.; Ivanova, S. *Spectrochim. Acta, Part A: Mol. Biomol. Spectrosc.* **2000**, *56A*, 409-416.
(29) Gallez, B.; Baudelet, C.; Debuyst, R. *J. Nutr.* **2000**, *130*, 1831–1833.